Rab27 effector Slp2-a transports the apical signaling molecule podocalyxin to the apical surface of MDCK II cells and regulates claudin-2 expression

Takao Yasuda[a], Chika Saegusa[b], Sachiko Kamakura[c], Hideki Sumimoto[c], and Mitsunori Fukuda[a]
[a]Laboratory of Membrane Trafficking Mechanisms, Department of Developmental Biology and Neurosciences, Graduate School of Life Sciences, Tohoku University, Aobayama, Aoba-ku, Sendai, Miyagi 980-8578, Japan; [b]Biomedicinal Information Research Center, National Institute of Advanced Industrial Science and Technology, 2-4-7 Aomi, Koto-ku, Tokyo 135-0064, Japan; [c]Department of Biochemistry, Kyushu University Graduate School of Medical Sciences, 3-1-1 Maidashi, Higashi-ku, Fukuoka 812-8582, Japan

ABSTRACT **Most cells in tissues are polarized and usually have two distinct plasma membrane domains—an apical membrane and a basolateral membrane, which are the result of polarized trafficking of proteins and lipids. However, the mechanism underlying the cell polarization is not fully understood. In this study, we investigated the involvement of synaptotagmin-like protein 2-a (Slp2-a), an effector molecule for the small GTPase Rab27, in polarized trafficking by using Madin–Darby canine kidney II cells as a model of polarized cells. The results show that the level of Slp2-a expression in MDCK II cells increases greatly as the cells become polarized and that its expression is specifically localized at the apical membrane. The results also reveal that Slp2-a is required for targeting of the signaling molecule podocalyxin to the apical membrane in a Rab27A-dependent manner. In addition, ezrin, a downstream target of podocalyxin, and ERK1/2 are activated in Slp2-a–knockdown cells, and their activation results in a dramatic reduction in the amount of the tight junction protein claudin-2. Because both Slp2-a and claudin-2 are highly expressed in mouse renal proximal tubules, Slp2-a is likely to regulate claudin-2 expression through trafficking of podocalyxin to the apical surface in mouse renal tubule epithelial cells.**

Monitoring Editor
Akihiko Nakano
RIKEN

Received: Feb 10, 2012
Revised: Jun 20, 2012
Accepted: Jun 25, 2012

INTRODUCTION

Cell polarity is a characteristic property of well-differentiated eukaryotic cells, and the physiological functions of polarized cells depend on the asymmetrical organization of cellular components, including the plasma membrane, organelles, and cytoskeletons. In epithelial cells—one of the most basic types of polarized cells—membranes and secretory proteins are delivered to specific regions of the plasma membrane, that is, the apical membrane and the basolateral membrane, which are separated by tight junctions, thereby defining and maintaining their unique identities and functions (Mostov *et al.*, 2003; Rodriguez-Boulan *et al.*, 2005; Rodríguez-Fraticelli *et al.*, 2011). During the past few decades, more and more proteins involved in polarized membrane trafficking have been identified. The proteins have included members of the Rab-type small GTPases, conserved membrane-trafficking proteins in all eukaryotes (Fukuda, 2008; Stenmark, 2009), and their effectors, but their precise role in polarized trafficking is poorly understood.

The *Drosophila* synaptotagmin-like protein (Slp) bitesize (Btsz), the only homologue of mammalian Slp with C-terminal tandem C2 domains (Fukuda *et al.*, 2001), has been reported to be localized apically (Serano and Rubin, 2003) and to be involved in maintenance

This article was published online ahead of print in MBoC in Press (http://www.molbiolcell.org/cgi/doi/10.1091/mbc.E12-02-0104) on July 5, 2012.

Address correspondence to: Mitsunori Fukuda (nori@m.tohoku.ac.jp).

Abbreviations used: AJR, apical junctional region; Btsz, bitesize; EGF, epidermal growth factor; EGFP, enhanced green fluorescent protein; EGFR, epidermal growth factor receptor; ERM, ezrin-radixin-moesin; GAPDH, glyceraldehyde 3-phosphate dehydrogenase; HRP, horseradish peroxidase; KD, knockdown; MAPK, mitogen-activated protein kinase; MDCK, Madin–Darby canine kidney; mRFP, monomeric red fluorescent protein; OA, okadaic acid; PBS, phosphate-buffered saline; PFA, paraformaldehyde; PP2A, protein phosphatase 2A; RT, reverse transcriptase; SHD, Slp homology domain; shRNA, short hairpin RNA; siRNA, small interfering RNA; Slp, synaptotagmin-like protein; TER, transepithelial electrical resistance.

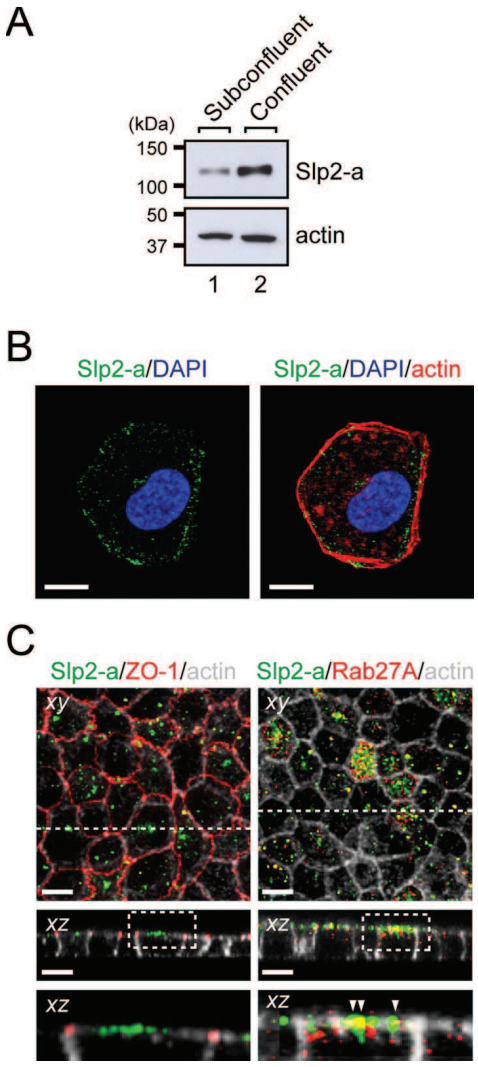

FIGURE 1: Slp2-a is localized at the apical membrane in polarized MDCK II cells. (A) Up-regulation of Slp2-a protein in confluent MDCK II cells. Total cell lysates of subconfluent and confluent MDCK II cells were subjected to immunoblot analysis with the antibodies indicated on the right. The level of Slp2-a expression in confluent MDCK II cells was much higher than in subconfluent MDCK II cells, whereas their level of actin expression was similar. The positions of the molecular mass markers (in kilodaltons) are shown on the left. (B) Localization of Slp2-a at the plasma membrane in a single MDCK II cell. MDCK II cells were transfected with pEGFP-C1-Slp2-a and cultured for 48 h. The transfected MDCK II cells were seeded on glass-bottomed dishes and cultured for 24 h. The cells were fixed, permeabilized, and stained with anti-GFP antibody (green) and Texas red–conjugated phalloidin (for actin staining; red). Note that Slp2-a dotted signals were observed near the plasma membrane, as well as in the cytoplasm of subconfluent MDCK II cells. Nuclei were stained with DAPI (blue). Scale bars, 10 μm. (C) Localization of Slp2-a together with Rab27A at the apical membrane in polarized MDCK II cells. Confluent MDCK II cells were fixed, permeabilized, and costained with anti–Slp2-a antibody (green), Alexa Fluor 633–conjugated phalloidin (gray), and anti–ZO-1 antibody (left; red) or anti-Rab27A antibody (right; red). Confocal *xy* and *xz* sections are shown. Top, an *xy* image; middle, an *xz* section at the broken line (*xz*) shown in the top; bottom, a magnified view of the dotted boxed area shown in the middle. Note that Slp2-a was localized at the apical membrane of confluent MDCK II cells and not at the tight junction labeled with anti–ZO-1 antibody (left). Slp2-a and its ligand Rab27A were partially colocalized at the apical membrane (yellow dots; arrowheads). Scale bars, 10 μm.

of the apical junctional region (AJR) of epithelial cells through recruitment to the AJR of moesin, one of the ezrin/radixin/moesin (ERM) family proteins that bind F-actin (Pilot *et al.*, 2006). Because of the failure to form a stable, continuous network of actin filaments in the absence of Btsz, E-cadherin is not properly stabilized at the AJR of *Drosophila* embryonic epithelia (Pilot *et al.*, 2006). Although there is no Btsz orthologue in mammals, since five homologous proteins, Slp1–5, have been reported to function as specific Rab27-binding proteins in secretory cells (Kuroda *et al.*, 2002; Fukuda, 2005), certain Slp family members may have functions in mammalian epithelial cells that are similar to those of Btsz. However, involvement of mammalian Slp family members in polarized trafficking in epithelial cells has never been investigated.

In this study, we used Madin–Darby canine kidney (MDCK) II cells as a model of polarized cells and investigated the involvement of Slp2-a, originally described as a Rab27 effector in melanocytes and in particular secretory cells (Kuroda and Fukuda, 2004; Saegusa *et al.*, 2006; Yu *et al.*, 2007; Holt *et al.*, 2008), in polarized trafficking. The results show that Slp2-a regulates apical trafficking of podocalyxin-containing vesicles in MDCK II cells together with Rab27A and that podocalyxin transported to the apical surface transduces intracellular signals to express the tight junction protein claudin-2. We discuss the possible function of Slp2-a in claudin-2 expression in mouse renal epithelial cells based on our findings.

RESULTS

Slp2-a is specifically localized at the apical membrane in polarized MDCK II cells

We first investigated the expression of Slp2-a protein in MDCK II cells before and after the establishment of cell polarity. Immunoblot analysis with anti-Slp2-a–specific antibody indicated the presence of a much higher level of Slp2-a protein expression in confluent MDCK II cells than in subconfluent MDCK II cells (Figure 1A, top, and Supplemental Figure S1A, second panel). Furthermore, the level of Slp2-a protein expression in confluent MDCK II cells decreased when they were incubated with a Ca^{2+}-chelating reagent to disrupt cell–cell interaction (Supplemental Figure S1B), suggesting a close correlation between the level of Slp2-a protein expression and cell polarization. By contrast, the levels of expression of other Slp family members in subconfluent and confluent MDCK II cells were similar (Supplemental Figure S1A). Next we investigated the subcellular localization of endogenous Slp2-a protein by performing an immunofluorescence analysis. Although we were unable to detect any specific immunoreactive signals of endogenous Slp2-a protein in subconfluent MDCK II cells, presumably because of its lower expression level, immunoreactive signals of exogenously expressed enhanced green fluorescent protein (EGFP)–tagged Slp2-a were observed in the cytoplasm of subconfluent MDCK II cells, as well as at their plasma membrane (Figure 1B). By contrast, in polarized MDCK II cells immunoreactive signals of endogenous Slp2-a protein were observed specifically at the apical membrane. Moreover, Slp2-a was partially colocalized with its ligand Rab27A at the apical plasma membrane (Kuroda *et al.*, 2002; Figure 1C, bottom right, arrowheads), suggesting that Slp2-a functions together with Rab27A at the apical membrane in polarized MDCK II cells.

Slp2-a regulates expression of the tight junction protein claudin-2

To investigate the role of Slp2-a in polarized MDCK II cells, we established two independent MDCK II cell lines with diminished Slp2-a expression by RNA interference technology using two different *Slp2-a* short hairpin RNAs (shRNAs; sites 1 and 2), which we named

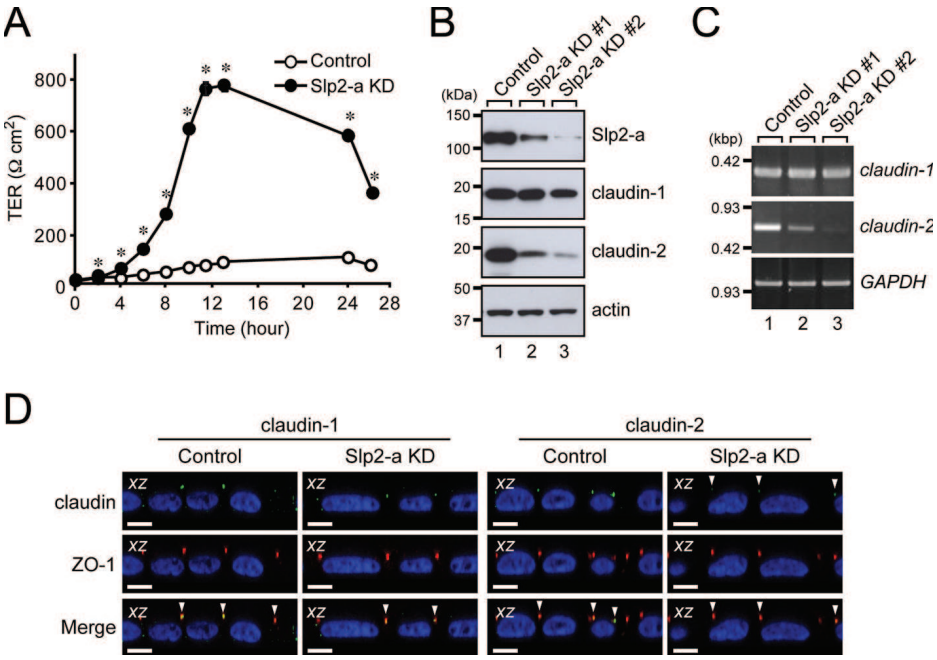

FIGURE 2: Claudin-2 expression in MDCK II cells is decreased in the absence of Slp2-a. (A) Increased TER of Slp2-a KD cells. TER was measured in confluent control cells and Slp2-a KD cells. The TER value of the Slp2-a KD cells was significantly higher than the TER value of the control cells. Data are expressed as the means ± SEM of three determinations. *$p < 0.01$ (Student's unpaired *t* test). (B) Decreased expression of claudin-2 protein in Slp2-a KD #1 and #2 cells. Total cell lysates of confluent control cells and Slp2-a KD #1/#2 cells were subjected to 10% SDS–PAGE, followed by immunoblotting with the antibodies indicated on the right. The level of claudin-2 protein expression in Slp2-a KD #1/#2 cells was much lower than in the control cells, whereas the level of claudin-1 protein expression appeared to be the same. Actin was used as an internal control. The positions of the molecular mass markers (in kilodaltons) are shown on the left. (C) Decreased expression of *claudin-2* mRNA in Slp2-a KD #1/#2 cells as revealed by RT-PCR analysis. Note that the level of *claudin-2* mRNA expression in Slp2-a KD #1/#2 cells, but not the level of *claudin-1* mRNA expression, was also dramatically decreased, the same as shown for claudin-2 protein expression in B. *GAPDH* was used as an internal control. The size of the molecular weight markers (kilobase pairs [kbp]) is shown on the left. (D) Correct targeting of claudin-2 to the tight junction in Slp2-a KD cells. Confluent control cells and Slp2-a KD cells were fixed, permeabilized, and stained with anti–ZO-1 antibody (red) and anti–claudin-1 antibody (left, green) or anti–claudin-2 antibody (right, green). Nuclei were stained with DAPI (blue). Confocal *xz* sections are shown. Although the intensity of claudin-2 staining was dramatically reduced in the Slp2-a KD cells, even in the absence of Slp2-a both claudin-1 and claudin-2 were correctly localized at the tight junction labeled with anti–ZO-1 antibody (yellow dots; bottom, arrowheads). Scale bars, 10 μm.

Slp2-a knockdown (KD) #1 cells and #2 cells, respectively. The levels of Slp2-a protein expression in Slp2-a KD #1 and #2 cells were 52.6 and 4.96%, respectively, of the level in parental MDCK II cells according to the results of an immunoblot analysis (Supplemental Figure S2A, lanes 3 and 4), whereas the level of Slp2-a protein expression in control shRNA MDCK II cells (simply referred to as control cells later), which had been stably transfected with an empty shRNA expression vector, was similar to the level in the parental MDCK II cells (Supplemental Figure S2A, lane 2). Because the level of Slp2-a protein expression in the Slp2-a KD #2 cells was reduced much more than in the Slp2-a KD #1 cells, we used Slp2-a KD #2 cells for the subsequent analyses (unless otherwise specified, "Slp2-a KD cells" means Slp2-a KD #2 cells throughout the rest of this article). Staining of Slp2-a KD cells with phalloidin and anti–ZO-1 antibody revealed the typical cobblestone-like appearance of epithelial cells, although the surface area of the cells was slightly increased (control cells, 287.3 ± 6.7 μm^2; Slp2-a KD cells, 448.4 ± 10.1 μm^2; $n = 70$ cells from four independent experiments; $p < 0.01$; Supplemental Figure S2B, *xy*). Moreover, there was no difference in the distribution of the apical marker syntaxin-3 or the basolateral marker E-cadherin between the control cells and the Slp2-a KD cells (Supplemental Figure S2B, *xz*, third and fourth panels), indicating that the steady-state distribution of polarized membrane markers in the Slp2-a KD cells is normal.

We then evaluated the barrier function of the Slp2-a KD cells by measuring transepithelial electrical resistance (TER). Of interest, confluent monolayers of the Slp2-a KD cells had markedly higher TER values than the control cells (Figure 2A). Because alteration of the pattern of expression of tight junction proteins, especially of claudin-2 (Furuse *et al.*, 2001), in MDCK cells has been shown to be related to different TER values, we investigated the protein expression of claudin-1 and claudin-2 by immunoblot analysis with specific antibodies. As expected, the level of claudin-2 protein expression was dramatically decreased in the Slp2-a KD cells, whereas the level of claudin-1 protein expression was the same as in the control cells (Figure 2B, second and third from top, lane 3). The claudin-2-deficiency in the Slp2-a KD cells is unlikely to have been attributable to off-target effects of the shRNAs, because a decreased claudin-2 protein level was also observed in another Slp2-a KD cell line (#1; Figure 2B, top and third from top, lane 2), and the level of claudin-2 protein expression was up-regulated by reexpression of an shRNA-resistant form of Slp2-a in the Slp2-a KD cells (Supplemental Figure S4, A and B). Note that the level of claudin-2 protein expression was proportional to the level of Slp2-a protein expression.

We proceeded to perform a reverse transcriptase (RT)-PCR analysis to determine whether the cause of the decreased level of claudin-2 protein expression was at the transcriptional level or at the translational level. As shown in Figure 2C, the level of *claudin-2* mRNA expression, but not of *claudin-1* mRNA expression, was dramatically decreased in both Slp2-a KD cell lines, indicating that Slp2-a is required for correct *claudin-2* mRNA expression. Because a small amount of claudin-2 protein was still present in the Slp2-a KD cells (Figure 2B), we also investigated its localization in the Slp2-a KD cells by an immunofluorescence analysis. To our surprise, claudin-2 protein was correctly localized at ZO-1–positive and claudin-1–positive tight junctions even in the Slp2-a KD cells (Figure 2D, far upper right, arrowheads); however, the intensity of the claudin-2 immunoreactive signals in the Slp2-a KD cells was markedly decreased in comparison with the control cells. Thus Slp2-a is unlikely to directly regulate trafficking of claudin-2 protein to tight junctions in MDCK II cells.

Apical membrane localization of Rab27A is Slp2-a dependent

Because Slp2-a and claudin-2 were differentially localized at the apical membrane and at the tight junction, respectively, we hypothesized

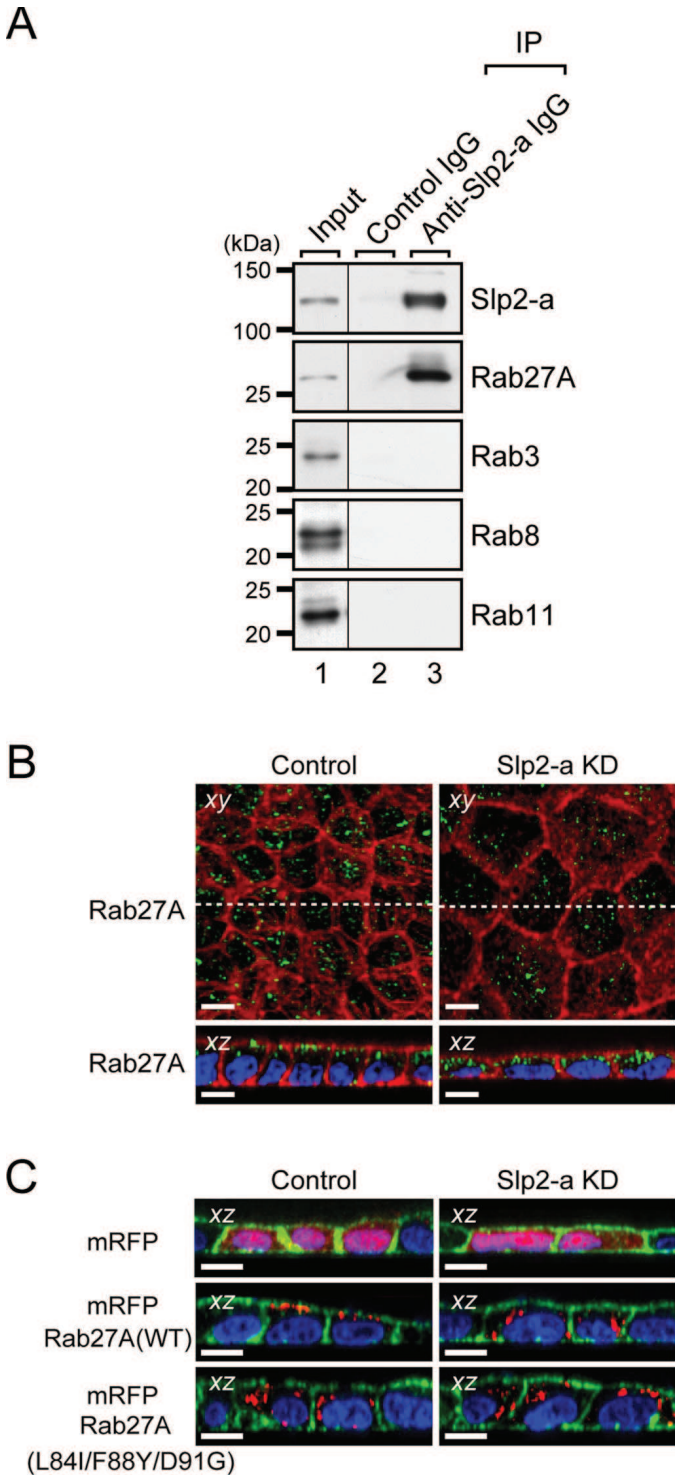

FIGURE 3: Slp2-a is required for the apical membrane localization of Rab27A in MDCK II cells. (A) Endogenous interaction between Slp2-a and Rab27A in MDCK II cells. Total cell lysates of confluent MDCK II cells were coimmunoprecipitated with anti–Slp2-a antibody and subjected to 10% SDS–PAGE, followed by immunoblotting with the antibodies indicated on the right. Note that Slp2-a interacted with Rab27A alone and not with any of the other Rabs tested. The positions of the molecular mass markers (in kilodaltons) are shown on the left. (B) Altered cellular localization of Rab27A in Slp2-a KD cells. Confluent control cells and Slp2-a KD cells were fixed, permeabilized, and stained with Texas red–conjugated phalloidin (red) and anti-Rab27A antibody (green). Although Rab27A was preferentially localized at the apical membrane in the control cells, the apical membrane localization of Rab27A was decreased in the Slp2-a KD cells. Nuclei were stained with DAPI (blue). Scale bars, 10 μm. (C) Requirement of Slp2-a binding of Rab27A for apical membrane localization. Control cells and Slp2-a KD cells were transfected with pmRFP-C1, pmRFP-C1-Rab27A(WT), or pmRFP-C1-Rab27A(L84I/F88Y/D91G). Two days after transfection, the cells were fixed, permeabilized, and stained with Alexa Fluor 488–conjugated phalloidin (green) and DAPI (blue). Although mRFP-Rab27A(WT) was preferentially localized at the apical membrane, the mutant protein was dispersed throughout the cytoplasm in the control cells (left, red). By contrast, both mRFP-Rab27A(WT) and mRFP-Rab27A(L84I/F88Y/D91G) were dispersed throughout the cytoplasm in the Slp2-a KD cells (right, red). Top, the cytosolic localization of control mRFP alone both in the control cells and in the Slp2-a KD cells. Scale bars, 10 μm.

that Slp2-a is involved in the apical trafficking of signaling molecules that induce *claudin-2* mRNA expression. Slp2-a has been shown to function as a Rab27 effector that mediates specific membrane-trafficking events, including melanosome transport, in particular cell types (Kuroda and Fukuda, 2004; Saegusa *et al.*, 2006; Yu *et al.*, 2007; Holt *et al.*, 2008), and thus it seemed highly possible that Slp2-a was also involved in the trafficking of Rab27-bearing vesicles to the apical membrane in MDCK II cells. To investigate this possibility, we performed coimmunoprecipitation assays with anti–Slp2-a (or anti-Rab27A) specific antibody in MDCK II cells (Figure 3A and Supplemental Figure S3A). Consistent with our previous reports (Kuroda *et al.*, 2002; Fukuda, 2006b), Slp2-a interacted with Rab27A alone and not with any of the other Rab proteins that were tested–for example, Rab3, Rab8, or Rab11—in MDCK II cells. The interaction between Slp2-a and Rab27A was also observed in mouse kidney (Supplemental Figure S3B). To further clarify the relationship between Slp2-a and Rab27A, we compared the subcellular localization of endogenous Rab27A protein in control cells and Slp2-a KD cells by an immunofluorescence analysis (Figure 3B). The results clearly showed that the apical membrane localization of Rab27A protein was dramatically decreased in the Slp2-a KD cells (hardly any green Rab27A signals were observed in Figure 3B, upper right, *xy*), whereas the apical membrane localization of endogenous syntaxin-3 protein and the intracellular localization of other Rab proteins, which cannot bind Slp2-a, were unaffected by the Slp2-a KD (Supplemental Figure S2B).

If Slp2-a were actually involved in the apical trafficking of Rab27-bearing vesicles, exogenously expressed Rab27A in the Slp2-a KD cells should not be targeted to the apical membrane. As expected, monomeric red fluorescent protein (mRFP)–tagged Rab27A did not exhibit apical membrane localization (i.e., scattered dots in the cytoplasm) in the Slp2-a KD cells, whereas the same protein clearly targeted to the apical membrane in the control cells (Figure 3C, middle). By contrast, a Rab27A(L84I/F88Y/D91G) mutant, which lacks critical residues for Rab27 effector binding in the switch II region (Fukuda, 2002, 2006a; Chavas *et al.*, 2008; Kukimoto-Niino *et al.*, 2008), was dispersed throughout the cytoplasm in both the control cells and the Slp2-a KD cells (Figure 3C, bottom). We also investigated the possible involvement of Rab27A in the regulation of claudin-2 expression by using two different *Rab27A* small interfering RNAs (siRNAs). As shown in Supplemental Figure S4, C and D, the level of claudin-2 protein expression was significantly decreased in Rab27A KD cells. However, the reduction in the amount of claudin-2 expression in Rab27A KD cells was not as evident (Supplemental Figure S4D) as it was in the Slp2-a KD cells (Figure 2B), even though there was a dramatic decrease in the level of Rab27A expression in Rab27A KD cells (Supplemental Figure S4C). This discrepancy may be explained by the compensatory effect of Rab27B, which can also

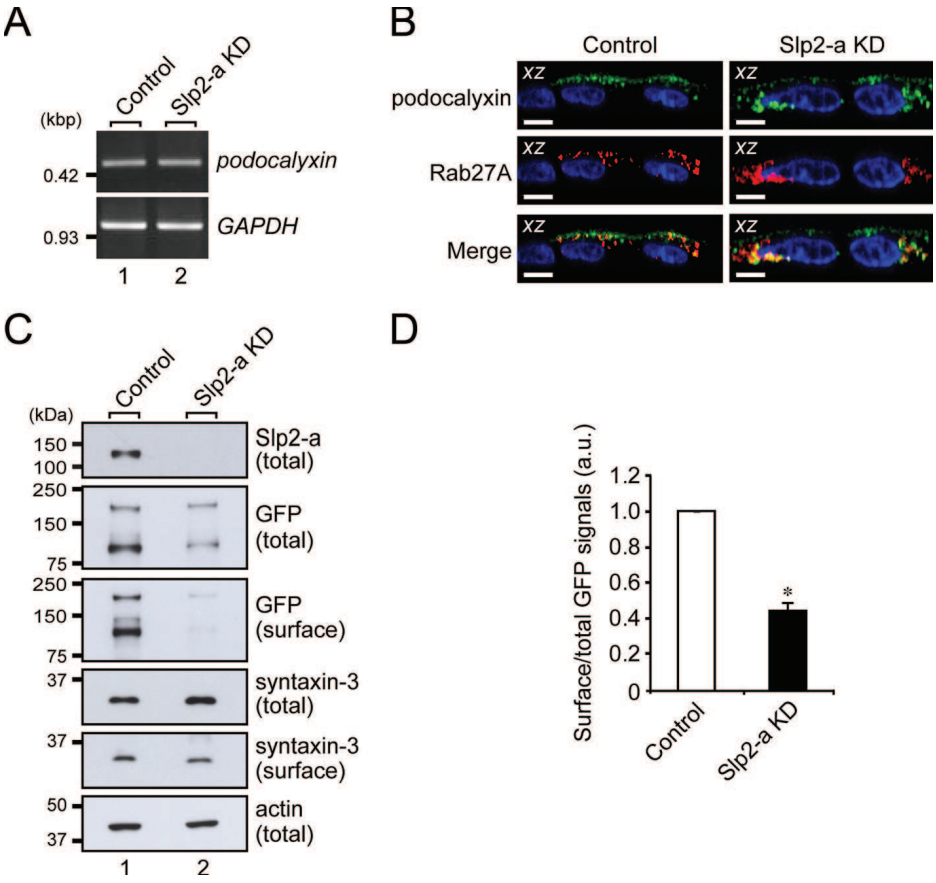

FIGURE 4: Slp2-a is involved in the apical targeting of podocalyxin in MDCK II cells. (A) Unaltered expression of *podocalyxin* mRNA in Slp2-a KD cells as demonstrated by RT-PCR analysis. The level of *podocalyxin* mRNA expression in the control cells and the Slp2-a KD cells was the same. *GAPDH* was used as an internal control. The size of the molecular weight markers (kilobase pairs [kbp]) is shown on the left. (B) Colocalization of Rab27A and podocalyxin in the intracellular compartment. Control cells and Slp2-a KD cells were transfected with a podocalyxin-Venus expression vector and pmRFP-C1-Rab27A, and 2 d after transfection, the cells were fixed, permeabilized, and stained with DAPI (blue). Podocalyxin (green) and Rab27A (red) were partially colocalized at the apical membrane and in the cytoplasm even in the absence of Slp2-a (yellow dots). Although podocalyxin (left, green) was preferentially localized at the apical membrane in the control cells, podocalyxin was dispersed throughout the cytoplasm in the Slp2-a KD cells (top right, green), the same as Rab27A protein was (middle right, red). Scale bars, 10 μm. (C) Reduced surface podocalyxin expression in Slp2-a KD cells. Control cells and Slp2-a KD cells were transfected with a podocalyxin-Venus expression vector, and 2 d after transfection, total cell lysates and surface biotinylated proteins were subjected to 10% SDS–PAGE, followed by immunoblotting with the antibodies indicated on the right. Actin was used as an internal control. The positions of the molecular mass markers (in kilodaltons) are shown on the left. (D) Quantification of GFP (podocalyxin-Venus) signals shown in C. Note that the level of podocalyxin-Venus expression at the apical membrane was significantly decreased in the absence of Slp2-a, whereas the level of syntaxin-3 at the apical membrane was about the same. Data are expressed as the means ± SEM of three independent experiments. *$p < 0.01$ (Student's unpaired *t* test). a.u., arbitrary units.

bind Slp2-a (Fukuda, 2006b), that is, Rab27B contributes to claudin-2 expression in Rab27A KD MDCK II cells (Supplemental Figure S4E). These results strongly indicated that Slp2-a is involved in the apical membrane targeting of Rab27A-bearing (and presumably Rab27B-bearing) vesicles in MDCK II cells via a direct interaction with Rab27A, as well as in the regulation of claudin-2 expression.

Slp2-a is required for the apical membrane targeting of podocalyxin in MDCK II cells

Next we searched the literature for candidate apical membrane proteins that induce claudin-2 expression and are transported to the apical membrane by Rab27-bearing vesicles. We focused on podocalyxin as a candidate signaling molecule because podocalyxin had been shown to be endogenously expressed (Meder *et al.*, 2005; Cheng *et al.*, 2005) and to alter TER when overexpressed (Takeda *et al.*, 2000) in MDCK II cells. Podocalyxin is also known to transduce signals, for example, RhoA, Rac, and mitogen-activated protein kinase (MAPK; Takeda, 2003; Schmieder *et al.*, 2004; Sizemore *et al.*, 2007; Hsu *et al.*, 2010), some of which are known to affect claudin-2 expression in MDCK II cells (Singh and Harris, 2004; Lipschutz *et al.*, 2005; Guillemot and Citi, 2006; Guillemot *et al.*, 2008; Flores-Benitez *et al.*, 2009; Ikari *et al.*, 2011). First, we performed an RT-PCR analysis to compare the level of *podocalyxin* mRNA expression in the control cells and the Slp2-a KD cells (Figure 4A). The RT-PCR analysis showed that *podocalyxin* mRNA was actually expressed in both the control cells and the Slp2-a KD cells and that the level of *podocalyxin* mRNA expression was similar in both of them. Next, to determine the subcellular localization of podocalyxin, we expressed C-terminal Venus (a variant of yellow fluorescent protein)-tagged podocalyxin in the control cells and the Slp2-a KD cells. As shown in Figure 4B (top), podocalyxin was localized at the apical membrane in the control cells, whereas the apical membrane localization of podocalyxin was dramatically decreased in the Slp2-a KD cells. Intriguingly, podocalyxin and Rab27A were colocalized in the cytoplasm of both the control cells and the Slp2-a KD cells (Figure 4B, bottom). The decreased apical membrane localization of podocalyxin was further confirmed biochemically by surface biotinylation assays, which showed that the surface expression of podocalyxin, but not of syntaxin-3, was significantly decreased in the Slp2-a KD cells (Figure 4, C and D). These results indicated that podocalyxin is the most likely candidate for the cargo of Rab27-bearing vesicles, whose targeting to the apical membrane is mediated by the function of the Slp2-a–Rab27A complex.

Ezrin, a downstream target of podocalyxin, is activated in the absence of Slp2-a

ERM family proteins act both as linkers between the actin cytoskeleton and plasma membrane proteins and as signal transducers in response to the stimuli that induce cytoskeletal remodeling (Bretscher *et al.*, 2002). Because ezrin has been shown to interact with podocalyxin (Takeda *et al.*, 2001; Orlando *et al.*, 2001; Schmieder *et al.*, 2004) and to be involved in the regulation of the RhoA, MAPK, and phosphoinositide 3-kinase signaling pathways (Schmieder *et al.*, 2004; Sizemore *et al.*, 2007), we focused on ezrin as a candidate molecule downstream of podocalyxin and

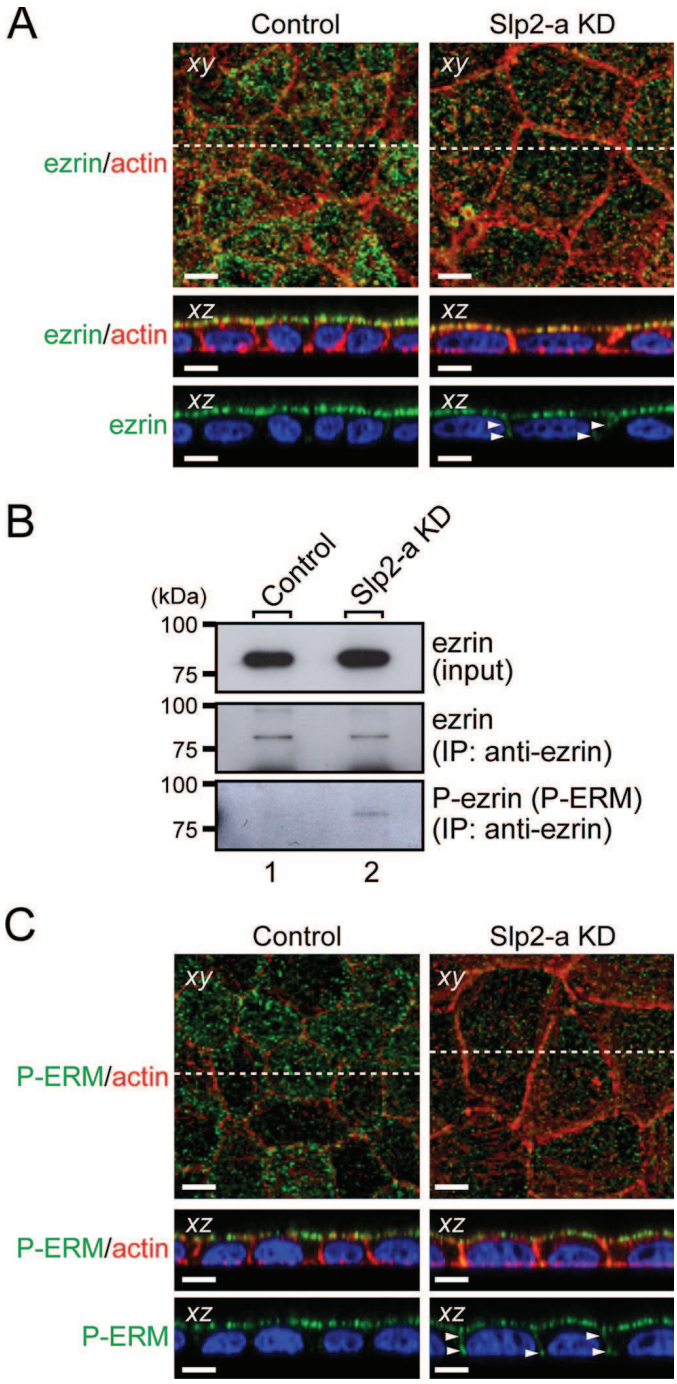

FIGURE 5: Ezrin, a downstream target of podocalyxin, is activated in Slp2-a KD cells. (A) Altered cellular localization of ezrin in Slp2-a KD cells. Confluent control cells and Slp2-a KD cells were fixed, permeabilized, and stained with anti-ezrin antibody (green) and Texas red–conjugated phalloidin (red). Ezrin was almost exclusively localized at the apical membrane in the control cells, whereas even though ezrin was preferentially localized at the apical region in the Slp2-a KD cells, ezrin was also localized at the basolateral membrane (arrowheads). Nuclei were stained with DAPI (blue). Scale bars, 10 μm. (B) Increased phosphorylation of ezrin in Slp2-a KD cells. Total cell lysates of confluent control cells and Slp2-a KD cells were immunoprecipitated with anti-ezrin antibody and subjected to 10% SDS–PAGE, followed by immunoblotting with the antibodies indicated on the right. The phosphorylation level of ezrin in the Slp2-a KD cells was much higher than in the control cells, whereas the level of ezrin expression appeared to be the same. The positions of the molecular mass markers (in kilodaltons) are shown on the left. (C) Phosphorylation of ERM proteins at the plasma membrane. Confluent control cells and Slp2-a KD cells were fixed, permeabilized, and stained with anti–phospho-ERM antibody (P-ERM; green) and Texas red–conjugated phalloidin (actin; red). Immunoreactive signals of phospho-ERM were observed at the apical membrane in the control cells, the same as those of ezrin, whereas in the Slp2-a KD cells immunoreactive signals of phospho-ERM were also observed at both the apical membrane and the basolateral membrane (arrowheads). Nuclei were stained with DAPI (blue). Scale bars, 10 μm.

investigated the subcellular localization of endogenous ezrin in the Slp2-a KD cells. Although ezrin was predominantly localized at the apical membrane in the control cells (Figure 5A, left), reduced immunoreactive ezrin signals were evident at the apical membrane, and some ectopic ezrin signals were also observed at the basolateral membrane in the Slp2-a KD cells (Figure 5A, right, arrowheads), indicating that ezrin fails to accumulate at the apical membrane in the Slp2-a KD cells because of the decreased apical membrane localization of podocalyxin. Because the altered intracellular localization of ezrin in the Slp2-a KD cells was assumed to affect its activity, we next explored the activity of ezrin, that is, phosphorylation of ezrin, by an immunoprecipitation analysis with anti-ezrin–specific antibody (Figure 5B). Unexpectedly, phosphorylation of ezrin was found to be increased in the Slp2-a KD cells in comparison with the control cells. Moreover, an immunofluorescence analysis with anti–phospho-ERM antibody showed that ERM proteins were phosphorylated at the apical membrane in the control cells, whereas they were phosphorylated at both the apical membrane and the basolateral membrane in the Slp2-a KD cells (Figure 5C, arrowheads), suggesting that the phosphorylation of ezrin at the basolateral membrane in the Slp2-a KD cells affects intracellular signal transduction.

Epidermal growth factor–independent MAPK signaling is activated in the absence of Slp2-a

Because the increased phosphorylation of ezrin has been shown to modulate signaling pathways, such as the MAPK pathway (Sizemore *et al.*, 2007), we analyzed the activity of the MAPK pathway by measuring the amount of phosphorylated, active ERK1/2. An immunoblot analysis showed that ERK1/2 phosphorylation was actually increased in the Slp2-a KD cells in comparison with the control cells (Figure 6A, middle). Given that it had been reported that activation of the MAPK pathway by epidermal growth factor (EGF) receptor (EGFR) activation decreases the mRNA and protein levels of claudin-2 (Singh and Harris, 2004; Lipschutz *et al.*, 2005; Flores-Benitez *et al.*, 2009; Ikari *et al.*, 2011), the increased activity of the MAPK pathway in the Slp2-a KD cells might have been attributable to the EGFR activation.

We therefore explored the level of EGFR protein expression by an immunoblot analysis with anti-EGFR antibody to investigate the involvement of EGF signaling in claudin-2 expression in the Slp2-a KD cells. However, both the total level and the surface expression level of EGFR protein were unaltered in the absence of Slp2-a (Figure 6B), indicating that Slp2-a is not involved in the apical targeting of EGFR. Furthermore, EGF treatment increased ERK1/2 phosphorylation and additively decreased the level of claudin-2 protein expression in both the control cells and the Slp2-a KD cells (Figure 6C, middle three panels), suggesting that increased ERK1/2 phosphorylation in the Slp2-a KD cells is induced by ezrin activation and not by activation of EGF signaling.

Slp2-a is expressed in mouse kidney

Claudin-2 is highly expressed in the tight junctions of mouse renal proximal tubules and is involved in the reabsorption of NaCl and

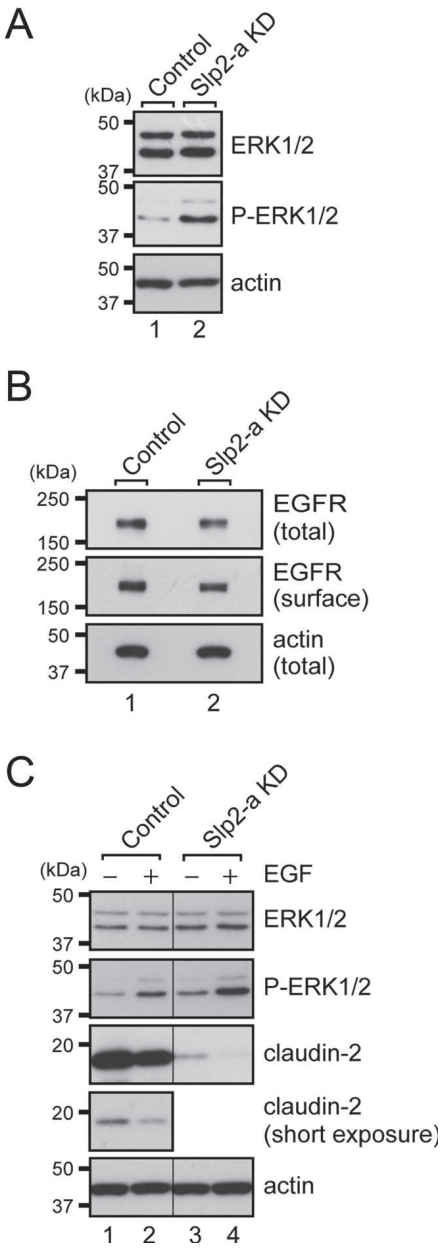

FIGURE 6: MAPK signaling is activated in Slp2-a KD cells independently of EGFR activation. (A) Increased phosphorylation of ERK1/2 in Slp2-a KD cells. Total cell lysates of confluent control cells and Slp2-a KD cells were subjected to 10% SDS–PAGE, followed by immunoblotting with the antibodies indicated on the right. Note that the phosphorylation level of ERK1/2 (P-ERK1/2) in the Slp2-a KD cells was markedly increased in comparison with the control cells, whereas the total level of ERK1/2 expression was the same. (B) Unaltered surface EGFR expression in Slp2-a KD cells. Total cell lysates and surface biotinylated proteins of confluent control cells and Slp2-a KD cells were subjected to 10% SDS–PAGE, followed by immunoblotting with the antibodies indicated on the right. Note that the level of EGFR expression and level of surface EGFR expression appeared to be the same. (C) Effect of EGF-stimulated EGFR activation. Confluent control cells and Slp2-a KD cells were treated with EGF for 16 h, and total cell lysates were subjected to 10% SDS–PAGE, followed by immunoblotting with the antibodies indicated on the right. Note that the ERK1/2 phosphorylation level in both the control cells and the Slp2-a KD cells was increased by EGF treatment and, as a result, that the level of claudin-2 expression was further decreased. Actin was used as an internal control. The positions of the molecular mass markers (in kilodaltons) are shown on the left.

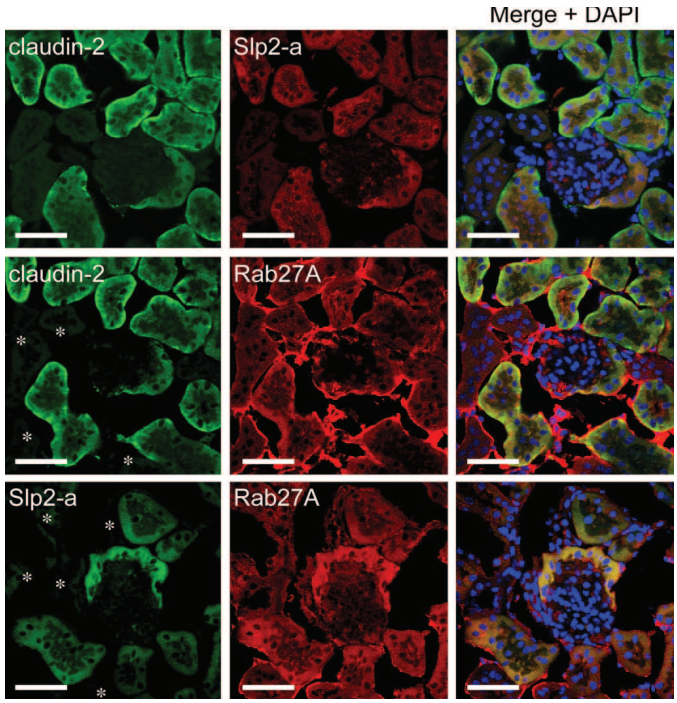

FIGURE 7: Slp2-a is expressed in mouse renal proximal tubules. The kidneys of female ICR mice were fixed, permeabilized, and stained with anti–Slp2-a antibody, anti–claudin-2 antibody, and/or anti-Rab27A antibody. Note that Slp2-a (red) and claudin-2 (green) were coexpressed in only the renal proximal tubules (top), whereas Rab27A (red) was expressed in all segments of the renal tubules and in the glomerulus (middle and bottom). Nuclei were stained with DAPI (right, blue). The asterisks indicate Rab27A-positive and claudin-2–negative or Slp2-a–negative sites. Scale bars, 50 μm.

water (Tsukita *et al.*, 2001; Kiuchi-Saishin *et al.*, 2002; Muto *et al.*, 2010). If Slp2-a is an upstream regulator of claudin-2 expression in mice, Slp2-a should be expressed in mouse renal proximal tubules, the same as claudin-2. Thus we stained mouse kidney with specific antibodies against Slp2-a, Rab27A, and claudin-2. The results of immunohistochemical analyses indicated that Slp2-a immunoreactive signals were present only in claudin-2–expressing tissue in mouse kidney (Figure 7, top), whereas Rab27A was expressed in all nephron segments (Figure 7, middle and bottom). Their coexpression in mouse renal proximal tubules suggested that Slp2-a regulates claudin-2 expression in mouse kidney, the same as in MDCK II cells.

DISCUSSION

Most organ systems (e.g., digestive, respiratory, genitourinary, and vascular systems) of multicellular animals are lined by a polarized monolayer of epithelial cells. The polarized epithelial cells have two surfaces—an apical surface that faces the lumen and a basolateral surface that is in contact with adjacent cells and the underlying connective tissue. These two surfaces are morphologically and functionally divided by tight junctions, which restrict the lateral diffusion of membrane proteins and lipids and function as a barrier between the cell and the extracellular milieu (Tsukita *et al.*, 2001; Bryant and Mostov, 2008). Thus elucidation of the polarized targeting machinery is important to understanding how cell polarity and morphology are maintained. In the present study, we identified Slp2-a as a novel apical trafficking protein in MDCK II cells. Slp2-a is localized at the apical membrane in polarized MDCK II cells (Figure 1C) and together with Rab27A regulates apical

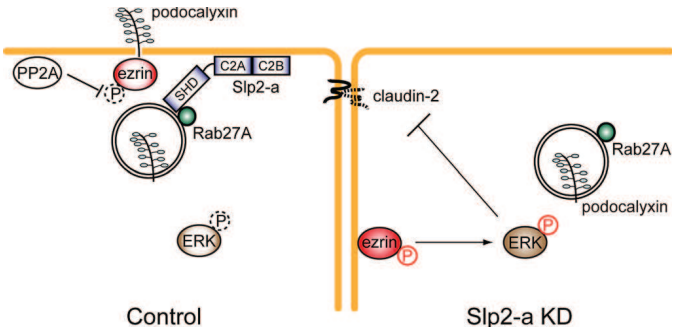

FIGURE 8: A model of claudin-2 expression in MDCK II cells through transport of podocalyxin to the apical surface by the function of the Slp2-a–Rab27A complex. In the control cells (left), podocalyxin-containing vesicles are docked/tethered at the apical membrane by the function of the Slp2-a–Rab27A complex. The apical membrane localization of Slp2-a is mediated by the phospholipid-binding activity of the C2A domain. Phosphorylated ezrin, which activates MAPK signals (Sizemore *et al.*, 2007), is recruited to and interacts with podocalyxin at the apical membrane, and ezrin is then dephosphorylated by phosphatase (e.g., PP2A) at the apical membrane (Nunbhakdi-Craig *et al.*, 2002; Zeidan *et al.*, 2008). As a result, phosphorylation of ERK1/2 is decreased and claudin-2 is expressed. By contrast, in the Slp2-a KD cells phosphorylated ezrin is ectopically localized at the basolateral membrane presumably because of the defect in podocalyxin trafficking to the apical membrane, and elevated ERK1/2 phosphorylation inhibits claudin-2 expression in the Slp2-a KD cells (right).

trafficking of podocalyxin-containing vesicles (Figure 4B). Bryant *et al.* (2010) reported that podocalyxin-containing vesicles are transported to the apical membrane through post-Golgi trafficking and a transcytosis pathway, in both of which Rab8 and Rab11 are involved. Given that Rab27A was partially colocalized with Rab8A and Rab11A (Supplemental Figure S5), it is tempting to speculate that the Slp2-a–Rab27A complex also regulates certain step of the post-Golgi trafficking and/or the transcytosis pathway. Because Slp2-a has a docking role of Rab27-bearing secretory vesicles (or melanosomes) in other cell types (Kuroda and Fukuda, 2004; Fukuda, 2006b), the Slp2-a–Rab27A complex is likely to regulate recruitment and docking of podocalyxin-containing vesicles to the apical membrane in MDCK II cells (Figure 8, control).

What is the function of the podocalyxin transported to the apical surface by the Slp2-a–Rab27A complex? Podocalyxin is a transmembrane sialomucin and has been shown to be involved in cell polarization and epithelial tubulogenesis (Rodríguez-Fraticelli *et al.*, 2011). Consistent with the previous reports that podocalyxin associates with ezrin (Takeda *et al.*, 2001; Orlando *et al.*, 2001; Schmieder *et al.*, 2004), apically localized endogenous ezrin was decreased in the absence of Slp2-a (Figure 5A). Our findings contrast somewhat with the previous finding in regard to the *Drosophila* Slp homologue Btsz, that is, moesin, the only member of the ERM protein family expressed in *Drosophila*, which is recruited to the AJR in a Btsz-dependent manner (Pilot *et al.*, 2006). Given that mammalian Slp2-a is not a direct orthologue of *Drosophila* Btsz, it is not surprising that Slp2-a regulates polarized trafficking in epithelial cells in a different manner from Btsz. We especially noted the structural difference between the two molecules: Slp2-a contains an N-terminal Slp homology domain (SHD or Rab27-binding domain) and Btsz does not (Fukuda *et al.*, 2001). Although Btsz is capable of being recruited to the AJR without an SHD (Pilot *et al.*, 2006), our detailed deletion and mutational analyses clearly indicated that the SHD is required for apical targeting of Slp2-a in MDCK II cells (Supplemental Figure S6A). Although the EGFP-tagged, full-length Slp2-a was clearly localized at the apical membrane, the same as endogenous Slp2-a protein (Supplemental Figure S6B, top left, green), the Slp2-a-ΔSHD mutant, which lacks an SHD, did not exhibit apical membrane localization, although it is localized at both the apical membrane and the basolateral membrane (Supplemental Figure S6B, left, third panel). In addition to the SHD, the phospholipid-binding activity of the C2A domain of Slp2-a is also required for its apical localization, because EGFP-C2A^{KQ} and EGFP-Slp2-a^{KQ} mutants, both of which lack the phospholipid-binding activity of the C2A domain as a result of neutralization of key Lys residues (Kuroda and Fukuda, 2004), failed to be localized at the plasma membrane (Supplemental Figure S6B, right). Another difference between Slp2-a and Btsz lies in their ERM recruitment mechanism: Slp2-a recruits ezrin to the apical membrane indirectly through trafficking of podocalyxin, which binds ezrin (Figures 5A and 8), whereas Btsz recruits moesin to the AJR directly (Pilot *et al.*, 2006). Actually, no interaction between mammalian Slp2-a and ezrin (or moesin) was observed in MDCK II cells under our immunoprecipitation conditions (unpublished data).

Although ezrin was decreased at the apical membrane in the Slp2-a KD cells (Figure 5A), we were surprised to find increased phosphorylation of ezrin in the absence of Slp2-a (Figure 5, B and C). Given that protein phosphatase 2A (PP2A) has been reported to be localized at the apical membrane in MDCK II cells (Nunbhakdi-Craig *et al.*, 2002), PP2A may dephosphorylate ezrin at the apical membrane (Zeidan *et al.*, 2008). In fact, when endogenous PP2A activity was inhibited by a specific PP2A inhibitor, okadaic acid (OA) (Haystead *et al.*, 1989), phosphorylation of ezrin was increased and claudin-2 expression was decreased even in the control cells (Supplemental Figure S7). Thus ezrin is likely to have been dephosphorylated by PP2A at the apical membrane in the control cells (Figure 8, control). This scenario seems plausible in the Slp2-a KD cells, because some ectopic phospho-ezrin immunoreactive signals at the basolateral membrane were observed in the Slp2-a KD cells but not in the control cells (Figure 5C, bottom right, arrowheads). These findings, together with the fact that activated ezrin is involved in the regulation of the MAPK pathway (Sizemore *et al.*, 2007), suggest that activation of the MAPK pathway (e.g., phosphorylation of ERK) by phospho-ezrin at the basolateral membrane inhibits claudin-2 expression (Figure 8, Slp2-a KD). Consistent with our model of ERK activation in Slp2-a KD cells, overexpression of a dominant-negative form of ERK(K52R) in Slp2-a KD cells clearly induced up-regulation of claudin-2 protein expression (Supplemental Figure S4, A and B). We also tried C-terminal–deleted ezrin, which has been reported to act as a dominant-negative form of ezrin (Ezrin-N; Bretscher *et al.*, 2002), but the C-terminal–deleted ezrin had no effect on claudin-2 expression in Slp2-a KD cells (T.Y. and M.F., unpublished data). Given that the phosphorylation level of ERK1/2 in the Slp2-a KD cells expressing the C-terminal–deleted ezrin was not significantly decreased (T.Y. and M.F., unpublished data), this mutant may not simply function as a dominant-negative mutant of ezrin in MDCK II cells. Alternatively, other downstream targets of podocalyxin might also be involved in the regulation of ERK1/2 phosphorylation.

In addition to MDCK II cells, we found that both Slp2-a and claudin-2 are coexpressed in mouse renal proximal tubules (Figure 7), and since podocalyxin is also expressed in renal tubules (Cheng *et al.*, 2005; Lin *et al.*, 2007), the same molecular mechanism regulated by Slp2-a and podocalyxin is likely to function in mouse renal proximal tubules. However, podocalyxin-deficient mice exhibit a severely impaired kidney development and die of anuric failure within 24 h after birth (Doyonnas *et al.*, 2001), whereas Slp2-a–deficient

mice are viable and fertile (Saegusa *et al.*, 2006). This discrepancy may be explained by the compensatory effect of Slp2-a-related proteins, such as Slp1, Slp2-b, Slp3-a, Slp4-a, and Slp5 (Fukuda, 2005, 2006b; Supplemental Figure S1A), in mice. Further work will be necessary to determine whether other Slp family members are also involved in the polarized trafficking that occurs in epithelial cells.

In conclusion, we demonstrated that Slp2-a is the first Slp member involved in polarized trafficking in mammalian epithelial cells, and we discovered that Slp2-a regulates apical targeting of podocalyxin and its binding partner ezrin in concert with Rab27A. In the absence of Slp2-a, the phospho-ezrin in MDCK II cells is ectopically localized at the basolateral membrane and then activates ERK by a largely unknown mechanism. The activated ERK then inhibits claudin-2 expression in the Slp2-a KD cells (a hypothetical model is summarized in Figure 8). Because previous studies on mammalian Slp family members have for the most part been limited to their secretory function—for example, exocytosis of hormones and enzymes—in secretory cells (Fukuda, 2006b, 2008), the findings in this study should provide a new paradigm for the function of Slp protein in the polarized trafficking of signaling molecules in epithelial cells.

MATERIALS AND METHODS

Materials

Horseradish peroxidase (HRP)–conjugated anti-GFP antibody was purchased from MBL (Nagoya, Japan). Anti-Rab3, anti-Rab8, anti-Rab11, anti-Rab27A, anti-moesin, and anti–E-cadherin mouse monoclonal antibodies were obtained from BD Transduction Laboratories (Lexington, KY). Anti–ZO-1 rat monoclonal antibody was from Chemicon International (Temecula, CA). Anti–claudin-1 and anti–claudin-2 rabbit polyclonal antibodies were from Invitrogen (Carlsbad, CA). Anti–syntaxin-3 rabbit polyclonal antibody was from Synaptic Systems (Göttingen, Germany). Anti-ezrin mouse monoclonal antibody was from Abcam (Cambridge, MA). Anti–phospho-ezrin(Thr-567)/radixin(Thr-564)/moesin(Thr-558)(anti–phospho-ERM) rabbit polyclonal antibody, anti–p44/42 MAPK (ERK1/2) rabbit polyclonal antibody, and anti–phospho-p44/42 (ERK1/2; Thr-202/Tyr-204) mouse monoclonal antibody were from Cell Signaling Technology (Danvers, MA). Anti-EGFR sheep polyclonal antibody was from Fitzgerald (Concord, MA). Anti-Slp1, anti–Slp2-a, anti–Slp3-a, and anti–Slp4-a rabbit polyclonal antibodies were prepared as described previously (Imai *et al.*, 2004). Two siRNAs against canine/human Rab27A site 1 (target site #1: 5′-GGAGAGGTTTCGTAGCTTA-3′) and site 2 (target site #2: 5′-CGACAGCGTTCTTCAGAGA-3′) were synthesized by Nippon EGT (Toyama, Japan).

Plasmid construction

pEGFP-C1 vectors (BD Biosciences Clontech, Palo Alto, CA) harboring mouse Slp2-a mutants or mouse Rab proteins and pmRFP-C1 vectors harboring mouse Rab27A mutants were prepared essentially as described previously (Kuroda and Fukuda, 2004; Fukuda, 2006a; Tsuboi and Fukuda, 2006). cDNA encoding human podocalyxin was amplified from Marathon-Ready adult human brain and testis cDNA (BD Biosciences Clontech) by PCR, with the following pairs of oligonucleotides having a restriction enzyme site (underlined) as described previously (Fukuda *et al.*, 1999): an N-terminal fragment (podocalyxin forward primer 1, 5′-GGATCCATGCGCTGCGCGCTGGCGCTCT-3′ and podocalyxin reverse primer 1, 5′-TATCGGTGGGTAGTTGATGCCTGCT-3′) and a C-terminal fragment (podocalyxin forward primer 2, 5′-AACGGCATTGAGAACACCTACCCT-3′ and podocalyxin reverse primer 2, 5′-GTCGACAGGTGTGTGTCTTCCTCCT-3′). To obtain full-length podocalyxin, each fragment was digested with appropriate restriction enzymes and then ligated. The resulting full-length podocalyxin cDNA was subcloned into the pVenus-N1 vector. cDNA encoding ERK2(K52R) was prepared according to the procedure described by Robinson *et al.* (1996) and subcloned into the pEF-FLAG tag expression vector (Fukuda *et al.*, 1999).

Cell culture, transfection, and EGF or OA treatment

MDCK II cells were cultured in DMEM (Sigma-Aldrich, St. Louis, MO) containing 10% fetal bovine serum, penicillin G (100 U/ml), and streptomycin (100 μg/ml). Plasmids were transfected into MDCK II cells by using Lipofectamine 2000 (Invitrogen) according to the manufacturer's instructions. For EGF treatment, MDCK II cells were cultured in serum-free DMEM medium for 6 h and then treated with EGF (100 ng/ml; Invitrogen) for 16 h. For OA treatment, confluent MDCK II cells were treated with OA (20 or 100 nM; LC Laboratories, Woburn, MA) for 16 h.

Establishment of Slp2-a–knockdown cell lines by RNA interference

pSilencer-control plasmids and pSilencer-canine Slp2-a (cSlp2-a) #1 and #2 plasmids (target site #1, 5′-GGATGAACTCCCACAGATT-3′, and target site #2, 5′-CGCTCAGATCCATATGTAA-3′) were transfected into MDCK II cells (1×10^5 cells) by using Lipofectamine 2000 as described. To establish cell lines stably expressing the pSilencer vectors, MDCK II cells were grown in DMEM containing 800 μg/ml G418 (Invitrogen). Stable MDCK II cells (referred to as control cells, Slp2-a KD #1 cells, and Slp2-a KD #2 cells, respectively) were plated on culture dishes, cultured for 72 h, and then subjected to immunoblotting and immunocytochemistry as described later.

Measurement of transepithelial electrical resistance

Stable MDCK II cells (4×10^5) were seeded on a Transwell filter (0.4-μm pore size; 12-mm diameter; Corning, Corning, NY) and grown to confluence in DMEM containing 1.8 mM Ca^{2+} (normal calcium medium). Cells were washed twice with phosphate-buffered saline (PBS; 137 mM NaCl, 2.7 mM KCl, 8.1 mM Na_2HPO_4, and 1.5 mM KH_2PO_4, pH 7.4) and incubated for 2 h in S-MEM (Invitrogen) containing 2.1 μM Ca^{2+} (low-calcium medium). TER was monitored with a Millicel-ERS volt-ohm meter (Millipore, Bedford, MA) immediately after the addition of the normal calcium medium DMEM (time 0) and at 90- to 120-min intervals for up to 26 h. TER values were calculated after subtracting the blank value (an empty filter) and expressed in ohm cm^2, as described by Matter and Balda (2003).

Preparation of total RNA and RT-PCR

Total RNA was prepared from stable MDCK II cells with TRI reagent (Sigma-Aldrich), and reverse transcription was performed by using a ReverTra Ace-kit (Toyobo, Osaka, Japan) according to the manufacturer's instructions. The canine glyceraldehyde 3-phosphate dehydrogenase (GAPDH), claudin-1, claudin-2, podocalyxin, and Rab27B primer pairs were designed to amplify fragments of 989, 307, 670, 506, and 657 base pairs, respectively. The primers were used for GAPDH (forward primer, 5′-ATGGTGAAGGTCGGAGTCAA-3′, and reverse primer, 5′-GCCATGTAGACCATGAGGTC-3′), claudin-1 (forward primer, 5′-ATTCAGTGCAAGGTCTTCGAC-3′, and reverse primer, 5′-GCCTGACCAAATTCATACCTG-3′), claudin-2 (forward primer, 5′-TTGTAGGCTACATCCTAGGC-3′, and reverse primer, 5′-CACACATACCCTGTCAGGCT-3′), podocalyxin (forward primer, 5′-CTCAAGATCAGTGCCATATA-3′, and reverse primer, 5′-TTAGAGGTGCGTGTCCTCCT-3′), and Rab27B (forward primer, 5′-ATGACCGATGGGGACTATGA-3′, and reverse primer, 5′-CTAACAGCCACATTTCTTCT-3′). cDNAs were amplified by PCR using rTaq DNA

polymerase (Toyobo) with 25 or 50 (for Rab27B) cycles of denaturation at 94°C for 0.5 min, annealing at 55°C for 0.5 min, and extension at 72°C for 1 min.

Immunofluorescence analysis

Stable MDCK II cells were cultured on glass-bottomed dishes (35-mm dish; MatTek, Ashland, MA) at (1–3) × 10^5 cells for 72 h and then fixed with 4% paraformaldehyde (PFA) for 10 min at room temperature. For immunostaining, cells were permeabilized with 0.3% Triton X-100 in PBS for 2 min and blocked with the blocking buffer (1% bovine serum albumin [BSA] and 0.1% Triton X-100 in PBS) for 1 h at room temperature. The cells were then incubated for 2 h at room temperature in the same buffer containing primary antibodies at the following concentrations: anti–Slp2-a antibody, 3 μg/ml; anti–ZO-1 antibody, 1/400 dilution; anti-moesin antibody, 1/100 dilution; anti–E-cadherin antibody, 1/100 dilution; anti-Rab8 antibody, 1/100 dilution; anti-Rab11 antibody, 1/100 dilution; anti-Rab27A antibody, 1/100 dilution; anti–claudin-1 antibody, 1/50 dilution; anti–claudin-2 antibody, 1/200 dilution; anti–syntaxin-3 antibody, 1/100 dilution; anti-ezrin antibody, 1/100 dilution; and anti–phospho-ERM antibody, 1/100 dilution. The cells were then incubated with secondary antibodies (Alexa 488–conjugated antibodies and Alexa 594–conjugated antibodies; Invitrogen) and 4′,6-diamidino-2-phenylindole (DAPI). To stain actin, cells were stained with Texas red–conjugated phalloidin or Alexa Fluor 488–conjugated phalloidin (each 1/100 dilution; Invitrogen). The stained cells were examined for immunofluorescence signals with a confocal fluorescence microscope (FluoView 1000; Olympus, Tokyo, Japan).

Immunoblot analysis

MDCK II cells were plated on 10-cm culture dishes at 2 × 10^5 cells and 2 × 10^6 cells, cultured for 48 h, and harvested as subconfluent cells and confluent cells, respectively. Parental MDCK II cells and stable MDCK II cells were plated on 6-cm dishes at (1–3) × 10^5 cells and cultured for 48 h. After rinsing the cells with PBS and lysing them in a lysis buffer (50 mM 4-(2-hydroxyethyl)-1-piperazineethanesulfonic acid [HEPES]–KOH, pH 7.2, 150 mM NaCl, 1 mM $MgCl_2$, 1% Triton X-100, and a protease inhibitor cocktail [Roche, Mannheim, Germany]), we subjected the lysates to 10% SDS–PAGE, followed by immunoblotting with the antibodies indicated in the figures. The intensity of the immunoreactive bands was quantified with ImageJ, version 1.44o (National Institutes of Health, Bethesda, MD). The blots shown in the figures are representative of three or four independent experiments.

Cell surface biotinylation assay

Biotinylation assays were performed essentially as described previously (Shin *et al.*, 2005). In brief, stable MDCK II cells grown on 10-cm dishes were transfected with podocalyxin-Venus expression vector and cultured for 48 h. Confluent MDCK II cells were washed three times with ice-cold PBS (+) (containing 0.1 mM $CaCl_2$ and 0.1 mM $MgCl_2$, pH 7.4) and incubated with 1 mg/ml Sulfo-NHS-LC-biotin (Pierce, Rockford, IL) in PBS (+) for 30 min on ice to biotinylate cell surface proteins. The reaction was quenched by washing the dishes twice with ice-cold PBS (+) containing 100 mM glycine and 0.3% (wt/vol) BSA, and the dishes were subsequently washed twice with PBS (+). The cells were then lysed in 1 ml of the previously described lysis buffer, and the lysates were centrifuged at 15,000 × g for 20 min at 4°C in a microcentrifuge to remove cellular debris and insoluble materials. The supernatant was incubated with streptavidin-agarose beads (Pierce) overnight at 4°C with constant rotation. The beads were then washed three times with the lysis buffer, twice with a high-salt wash buffer (50 mM Tris-HCl, pH 7.5, 500 mM NaCl, and 0.1% Triton X-100), and, finally, once with 50 mM Tris-HCl, pH 7.5. The proteins were eluted from the beads by boiling in 30 μl of the SDS sample buffer, separated by 10% SDS–PAGE, and analyzed by immunoblotting with HRP-conjugated anti-GFP antibody, anti–sytanxin-3 antibody, and anti-EGFR antibody.

Immunoprecipitation assay

Stable MDCK II cells were plated on 10-cm culture dishes at (1–3) × 10^6 cells and cultured for 48 h. The cells were rinsed with PBS and lysed in the lysis buffer containing a protease inhibitor cocktail (Sigma-Aldrich). The homogenate was rotated for 30 min at 4°C for solubilization, and the insoluble material was removed by centrifugation at 15,000 × *g* for 20 min at 4°C. The supernatant was incubated with 1 μg/ml anti-ezrin antibody for 3 h at 4°C or with 1 μg/ml anti–Slp2-a antibody (or anti-Rab27A antibody) for 16 h at 4°C with constant rotation and then with protein G–Sepharose beads or protein A–Sepharose beads (GE Healthcare, Little Chalfont, United Kingdom) for 1 h at 4°C. After washing the beads with the lysis buffer, we subjected the immunoprecipitates to 10% SDS–PAGE, followed by immunoblotting with anti-ezrin antibody and anti–phospho-ERM antibody. Mouse kidney, including renal epithelial cells, was similarly lysed in the foregoing lysis buffer, and the lysates were subjected to coimmunoprecipitation assays with anti-Rab27A antibody.

Immunohistological analysis

Immunohistochemical staining was performed essentially as described previously (Yasuda *et al.*, 2010). In brief, the kidneys were removed from female ICR mice and immersion fixed in 4% PFA in 0.1 M phosphate buffer (pH 7.4) for 16 h at room temperature. The fixed kidneys were equilibrated at 4°C in 10% sucrose in PBS for 8 h and then in 20% sucrose in PBS overnight. They were then embedded in Tissue-Tek O.C.T. compound (Sakura, Tokyo, Japan) and frozen at −80°C until used. The frozen kidneys were cut into 10-μm sections in a cryostat (Carl Zeiss, Jena, Germany) and transferred to microscope slides (Matsunami Glass, Osaka, Japan). The samples were permeabilized with 0.3% Triton X-100 for 1 h at room temperature and then stained with anti–Slp2-a antibody, anti–claudin-2 antibody, and anti-Rab27A antibody. To double stain for Slp2-a and claudin-2, we directly labeled Slp2-a antibody with Alexa Fluor 594 by using a direct labeling kit (Zenon Alexa Fluor 594 rabbit immunoglobulin G labeling kit; Invitrogen). The immunostained sections were examined with a confocal fluorescence microscope.

ACKNOWLEDGMENTS

We thank Megumi Aizawa for technical assistance and members of the Fukuda Laboratory for valuable discussions. This work was supported in part by Grants-in-Aid for Scientific Research from the Ministry of Education, Culture, Sports, and Technology of Japan (to M.F.).

REFERENCES

Bretscher A, Edwards K, Fehon RG (2002). ERM proteins and merlin: integrators at the cell cortex. Nat Rev Mol Cell Biol 3, 586–599.

Bryant DM, Datta A, Rodríguez-Fraticelli AE, Peränen J, Martin-Belmonte F, Mostov KE (2010). A molecular network for *de novo* generation of the apical surface and lumen. Nat Cell Biol 12, 1035–1045.

Bryant DM, Mostov KE (2008). From cells to organs: building polarized tissue. Nat Rev Mol Cell Biol 9, 887–901.

Chavas LMG, Ihara K, Kawasaki M, Torii S, Uejima T, Kato R, Izumi T, Wakatsuki S (2008). Elucidation of Rab27 recruitment by its effectors: structure of Rab27a bound to exophilin4/Slp2-a. Structure 16, 1468–1477.

Cheng HY *et al.* (2005). Molecular identification of canine podocalyxin-like protein 1 as a renal tubulogenic regulator. J Am Soc Nephrol 16, 1612–1622.
Doyonnas R, Kershaw DB, Duhme C, Merkens H, Chelliah S, Graf T, McNagny KM (2001). Anuria, omphalocele, and perinatal lethality in mice lacking the CD34-related protein podocalyxin. J Exp Med 194, 13–27.
Flores-Benitez D, Rincon-Heredia R, Razgado LF, Larre I, Cereijido M, Contreras RG (2009). Control of tight junctional sealing: roles of epidermal growth factor and prostaglandin E2. Am J Physiol Cell Physiol 297, C611–C620.
Fukuda M (2002). Synaptotagmin-like protein (Slp) homology domain 1 of Slac2-a/melanophilin is a critical determinant of GTP-dependent specific binding to Rab27A. J Biol Chem 277, 40118–40124.
Fukuda M (2005). Versatile role of Rab27 in membrane trafficking: focus on the Rab27 effector families. J Biochem 137, 9–16.
Fukuda M (2006a). Distinct Rab27A binding affinities of Slp2-a and Slac2-a/melanophilin: hierarchy of Rab27A effectors. Biochem Biophys Res Commun 343, 666–674.
Fukuda M (2006b). Rab27 and its effectors in secretory granule exocytosis: a novel docking machinery composed of a Rab27·effector complex. Biochem Soc Trans 34, 691–695.
Fukuda M (2008). Regulation of secretory vesicle traffic by Rab small GTPases. Cell Mol Life Sci 65, 2801–2813.
Fukuda M, Kanno E, Mikoshiba K (1999). Conserved N-terminal cysteine motif is essential for homo- and heterodimer formation of synaptotagmins III, V, VI, and X. J Biol Chem 274, 31421–31427.
Fukuda M, Saegusa C, Mikoshiba K (2001). Novel splicing isoforms of synaptotagmin-like proteins 2 and 3: identification of the Slp homology domain. Biochem Biophys Res Commun 283, 513–519.
Furuse M, Furuse K, Sasaki H, Tsukita S (2001). Conversion of *zonulae occludentes* from tight to leaky strand type by introducing claudin-2 into Madin-Darby canine kidney I cells. J Cell Biol 153, 263–272.
Guillemot L, Citi S (2006). Cingulin regulates claudin-2 expression and cell proliferation through the small GTPase RhoA. Mol Biol Cell 17, 3569–3577.
Guillemot L, Paschoud S, Jond L, Foglia A, Citi S (2008). Paracingulin regulates the activity of Rac1 and RhoA GTPases by recruiting Tiam1 and GEF-H1 to epithelial junctions. Mol Biol Cell 19, 4442–4453.
Haystead TAJ, Sim ATR, Carling D, Honnor RC, Tsukitani Y, Cohen P, Hardie DG (1989). Effects of the tumour promoter okadaic acid on intracellular protein phosphorylation and metabolism. Nature 337, 78–81.
Holt O, Kanno E, Bossi G, Booth S, Daniele T, Santoro A, Arico M, Saegusa C, Fukuda M, Griffiths GM (2008). Slp1 and Slp2-a localize to the plasma membrane of CTL and contribute to secretion from the immunological synapse. Traffic 9, 446–457.
Hsu YH, Lin WL, Hou YT, Pu YS, Shun CT, Chen CL, Wu YY, Chen JY, Chen TH, Jou TS (2010). Podocalyxin EBP50 ezrin molecular complex enhances the metastatic potential of renal cell carcinoma through recruiting Rac1 guanine nucleotide exchange factor ARHGEF7. Am J Pathol 176, 3050–3061.
Ikari A, Takiguchi A, Atomi K, Sugatani J (2011). Epidermal growth factor increases clathrin-dependent endocytosis and degradation of claudin-2 protein in MDCK II cells. J Cell Physiol 226, 2448–2456.
Imai A, Yoshie S, Nashida T, Shimomura H, Fukuda M (2004). The small GTPase Rab27B regulates amylase release from rat parotid acinar cells. J Cell Sci 117, 1945–1953.
Kiuchi-Saishin Y, Gotoh S, Furuse M, Takasuga A, Tano Y, Tsukita S (2002). Differential expression patterns of claudins, tight junction membrane proteins, in mouse nephron segments. J Am Soc Nephrol 13, 875–886.
Kukimoto-Niino M, Sakamoto A, Kanno E, Hanawa-Suetsugu K, Terada T, Shirouzu M, Fukuda M, Yokoyama S (2008). Structural basis for the exclusive specificity of Slac2-a/melanophilin for the Rab27 GTPases. Structure 16, 1478–1490.
Kuroda TS, Fukuda M (2004). Rab27A-binding protein Slp2-a is required for peripheral melanosome distribution and elongated cell shape in melanocytes. Nat Cell Biol 6, 1195–1203.
Kuroda TS, Fukuda M, Ariga H, Mikoshiba K (2002). The Slp homology domain of synaptotagmin-like proteins 1–4 and Slac2 functions as a novel Rab27A binding domain. J Biol Chem 277, 9212–9218.
Lin WL, Pang VF, Liu CH, Chen JY, Shen KF, Lin YY, Yu CY, Hsu YH, Jou TS (2007). Pleomorphic extra-renal manifestation of the glomerular podocyte marker podocalyxin in tissues of normal beagle dogs. Histochem Cell Biol 127, 399–414.
Lipschutz JH, Li S, Arisco A, Balkovetz DF (2005). Extracellular signal-regulated kinases 1/2 control claudin-2 expression in Madin-Darby canine kidney strain I and II cells. J Biol Chem 280, 3780–3788.
Matter K, Balda MS (2003). Functional analysis of tight junctions. Methods 30, 228–234.
Meder D, Shevchenko A, Simons K, Fullekrug J (2005). Gp135/podocalyxin and NHERF-2 participate in the formation of a preapical domain during polarization of MDCK cells. J Cell Biol 168, 303–313.
Mostov K, Su T, ter Beest M (2003). Polarized epithelial membrane traffic: conservation and plasticity. Nat Cell Biol 5, 287–293.
Muto S *et al.* (2010). Claudin-2-deficient mice are defective in the leaky and cation-selective paracellular permeability properties of renal proximal tubules. Proc Natl Acad Sci USA 107, 8011–8016.
Nunbhakdi-Craig V, Machleidt T, Ogris E, Bellotto D, White CL III, Sontag E (2002). Protein phosphatase 2A associates with and regulates atypical PKC and the epithelial tight junction complex. J Cell Biol 158, 967–978.
Orlando RA, Takeda T, Zak B, Schmieder S, Benoit VM, McQuistan T, Furthmayr H, Farquhar MG (2001). The glomerular epithelial cell anti-adhesin podocalyxin associates with the actin cytoskeleton through interactions with ezrin. J Am Soc Nephrol 12, 1589–1598.
Pilot F, Philippe JM, Lemmers C, Lecuit T (2006). Spatial control of actin organization at adherens junctions by a synaptotagmin-like protein Btsz. Nature 442, 580–584.
Robinson MJ, Harkins PC, Zhang J, Baer R, Haycock JW, Cobb MH, Goldsmith EJ (1996). Mutation of position 52 in ERK2 creates a nonproductive binding mode for adenosine 5′-triphosphate. Biochemistry 35, 5641–5646.
Rodriguez-Boulan E, Kreitzer G, Müsch A (2005). Organization of vesicular trafficking in epithelia. Nat Rev Mol Cell Biol 6, 233–247.
Rodríguez-Fraticelli AE, Gálvez-Santisteban, Martin-Belmonte F (2011). Divide and polarize: recent advances in the molecular mechanism regulating epithelial tubulogenesis. Curr Opin Cell Biol 23, 638–646.
Saegusa C, Tanaka T, Tani S, Itohara S, Mikoshiba K, Fukuda M (2006). Decreased basal mucus secretion by Slp2-a-deficient gastric surface mucous cells. Genes Cells 11, 623–631.
Schmieder S, Nagai M, Orlando RA, Takeda T, Farquhar MG (2004). Podocalyxin activates RhoA and induces actin reorganization through NHERF1 and Ezrin in MDCK cells. J Am Soc Nephrol 15, 2289–2298.
Serano J, Rubin GM (2003). The *Drosophila* synaptotagmin-like protein bitesize is required for growth and has mRNA localization sequences within its open reading frame. Proc Natl Acad Sci USA 100, 13368–13373.
Shin HW, Kobayashi H, Kitamura M, Waguri S, Suganuma T, Uchiyama Y, Nakayama K (2005). Roles of ARFRP1 (ADP-ribosylation factor-related protein 1) in post-Golgi membrane trafficking. J Cell Sci 118, 4039–4048.
Singh AB, Harris RC (2004). Epidermal growth factor receptor activation differentially regulates claudin expression and enhances transepithelial resistance in Madin-Darby canine kidney cells. J Biol Chem 279, 3543–3552.
Sizemore S, Cicek M, Sizemore N, Ng KP, Casey G (2007). Podocalyxin increases the aggressive phenotype of breast and prostate cancer cells in vitro through its interaction with ezrin. Cancer Res 67, 6183–6191.
Stenmark H (2009). Rab GTPases as coordinators of vesicle traffic. Nat Rev Mol Cell Biol 10, 513–525.
Takeda T (2003). Podocyte cytoskeleton is connected to the integral membrane protein podocalyxin through Na^+/H^+-exchanger regulatory factor 2 and ezrin. Clin Exp Nephrol 7, 260–269.
Takeda T, Go WY, Orlando RA, Farquhar MG (2000). Expression of podocalyxin inhibits cell-cell adhesion and modifies junctional properties in Madin-Darby canine kidney cells. Mol Biol Cell 11, 3219–3232.
Takeda T, McQuistan T, Orlando RA, Farquhar MG (2001). Loss of glomerular foot processes is associated with uncoupling of podocalyxin from the actin cytoskeleton. J Clin Invest 108, 289–301.
Tsuboi T, Fukuda M (2006). Rab3A and Rab27A cooperatively regulate the docking step of dense-core vesicle exocytosis in PC12 cells. J Cell Sci 119, 2196–2203.
Tsukita S, Furuse M, Itoh M (2001). Multifunctional strands in tight junctions. Nat Rev Mol Cell Biol 2, 285–293.
Yasuda T *et al.* (2010). Rim2α determines docking and priming states in insulin granule exocytosis. Cell Metab 12, 117–129.
Yu M, Kasai K, Nagashima K, Torii S, Yokota-Hashimoto H, Okamoto K, Takeuchi T, Gomi H, Izumi T (2007). Exophilin4/Slp2-a targets glucagon granules to the plasma membrane through unique Ca^{2+}-inhibitory phospholipid-binding activity of the C2A domain. Mol Biol Cell 18, 688–696.
Zeidan YH, Jenkins RW, Hannun YA (2008). Remodeling of cellular cytoskeleton by the acid sphingomyelinase/ceramide pathway. J Cell Biol 181, 335–350.